

Supplementary information

CRISPR/Cas12a-Powered Nanoconfined Biosensing Platform with Hybrid Chain Reaction Cascading Guanine Nanowire Amplification for Ultrasensitive Dual-Mode Detection of Lipopolysaccharide

Yanlei Li^a, Xiang Ren^a, Dan Wu^a, Hongmin Ma^a, Qin Wei^a, Huangxian Ju^{a,b}, Zhongfeng Gao^{a*}

^a Key Laboratory of Interfacial Reaction & Sensing Analysis in Universities of Shandong, School of Chemistry and Chemical Engineering, University of Jinan, Jinan 250022, P. R. China.

^b State Key Laboratory of Analytical Chemistry for Life Science, Department of Chemistry, Nanjing University, Nanjing 210023, P. R. China.

*Corresponding authors

E-mail addresses: chm_gaozf@ujn.edu.cn (Zhongfeng Gao).

Contents

| | |
|---|-----|
| Reagents..... | S3 |
| Apparatus..... | S4 |
| Fig.S1 SEM characterization of VMSM. | S5 |
| Fig. S2 ECL intensity with the assembly time of the amplification process..... | S6 |
| Fig. S3 FL intensity with the assembly time of the amplification process..... | S7 |
| Fig. S4 ECL intensity under different pH of Tris-HCl..... | S8 |
| Fig. S5 FL intensity under different pH of Tris-HCl..... | S9 |
| Fig. S6 The stability of the biosensor was tested under different LPS concentrations with three parallel measurements. | S10 |
| Fig. S7 Selectivity test under different substance interference..... | S11 |
| Fig. S8 Selectivity test under different substance interference..... | S12 |
| Fig. S9 Reproducibility of the ECL response to 0.01 ng/mL LPS spiked..... | S13 |
| Fig. S10 Reproducibility of the FL response to 0.01 ng/mL LPS spiked..... | S14 |
| Table S1 Synthetic oligonucleotide sequences..... | S15 |
| Table S2. Comparison of LPS analysis using other methods with the proposed dual-mode detection. | S16 |
| Notes and references..... | S17 |

Reagents

Magnesium chloride, sodium chloride, potassium chloride, hydrochloric acid, sodium nitrate, sodium nitrite, tripropylamin, Tris(2,2'-bipyridine) ruthenium(II) hexahydrate, and anhydrous ethanol were procured from Sinopharm Chemical Reagent Co., Ltd. (Shanghai, China). Lipopolysaccharide and diethyl pyrocarbonate (DEPC) water were obtained from Sigma-Aldrich (St. Louis, MO, USA). 3-Aminopropyltriethoxysilane, tetraethoxysilane, hexadecyl trimethyl ammonium bromide, and phosphate-buffered saline were sourced from Macklin Reagent Co., Ltd. (Shanghai, China). Tris(hydroxymethyl)aminomethane hydrochloride buffer solution (Tris-HCl buffer), 4S GelRed, and all oligonucleotides were synthesized and acquired from Sangon Biotech (Shanghai, China), and purified using either 20.0% denaturing polyacrylamide gel electrophoresis or high-performance liquid chromatography (HPLC). All oligonucleotides were dissolved to a concentration of 100.0 μ M and stored at -20.0 °C. The DNA sequences are detailed in Table S1.

Apparatus

Scanning electron microscope (SEM) images were obtained using a field emission scanning electron microscope (Zeiss, Germany) to characterize the morphologies of the prepared nanomaterials. Transmission electron microscope (TEM) images were acquired from a JEM microscope (Hitachi, Japan). X-ray powder diffraction (XRD) patterns of the materials were obtained using an X-ray diffractometer (Tokyo, Japan) with $\text{CuK}\alpha$ radiation (40 kV, 300 mA) at a wavelength of 0.154 nm, as described by the Bragg equation: $2d \sin \theta = n\lambda$ (where $n = 1$ and $\lambda = 0.154$ nm). Fourier transform infrared spectroscopy (FT-IR) spectra were recorded using a VERTEX70 spectrometer (Bruker Co., Germany). UV-vis absorbance spectra were examined with a Lambda 25 UV-vis spectrophotometer (PerkinElmer, USA). Elemental analysis was performed using X-ray photoelectron spectroscopy (XPS, ESCALAB MK II, UK). ECL emission spectra were recorded on a custom-built ECL spectrum analyzer, which included a multichannel optical analyzer (SpectraPro300i, Acton Research Company) and a CHI 832 analyzer (Shanghai CHI Instruments, China). ECL signals were measured using an MPI-E electrochemiluminescence analyzer (Xi'an Remex Electronic Science Tech. Co., Ltd., China). Cyclic voltammetry (CV) and electrochemical impedance spectroscopy (EIS) measurements were conducted using an electrochemical workstation (Zahner Zennium PP211, Germany).

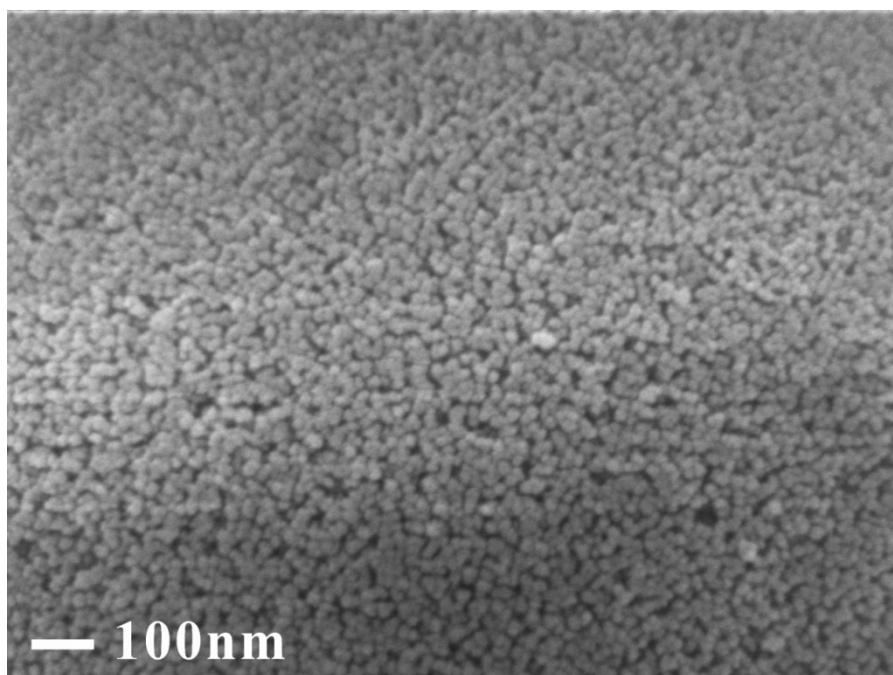


Fig.S1 SEM characterization of VMSM.

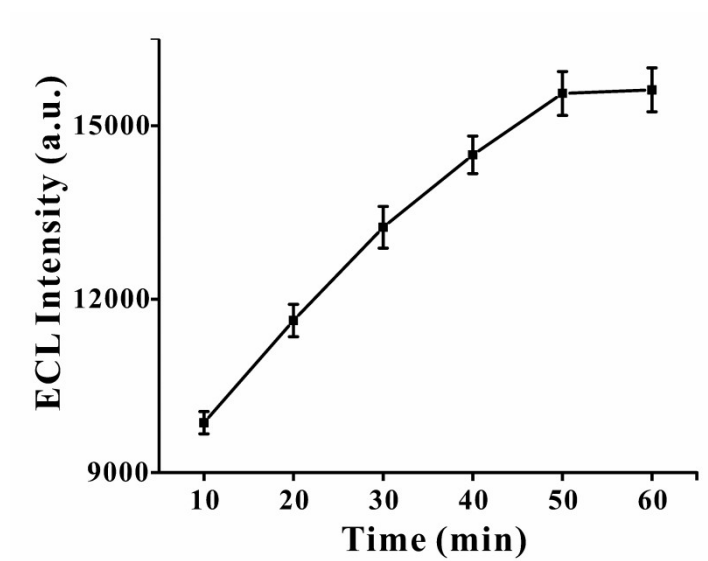


Fig. S2 ECL intensity with the assembly time of the amplification process. Error bars: SD ($n = 5$).

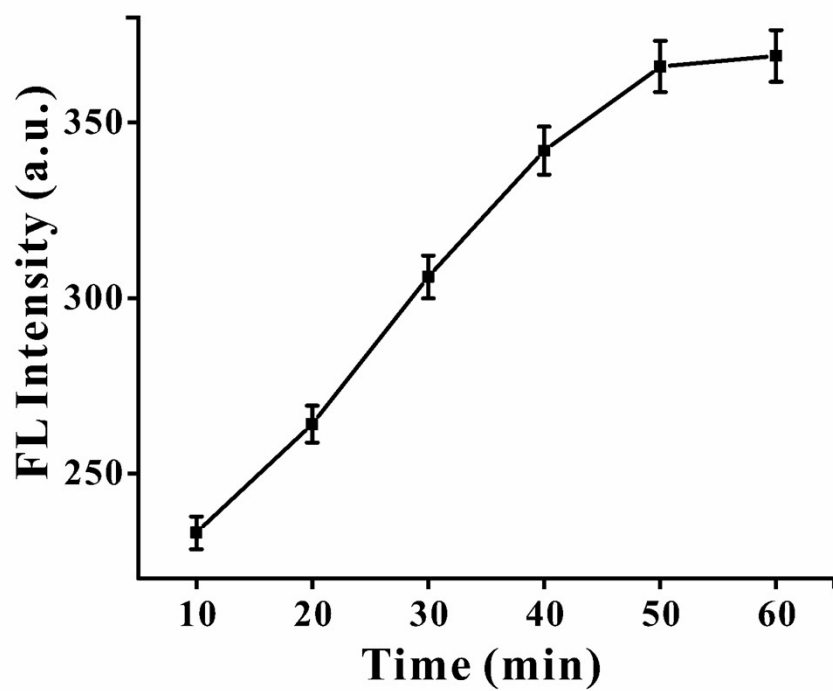


Fig. S3 FL intensity with the assembly time of the amplification process. Error bars: SD ($n = 5$).

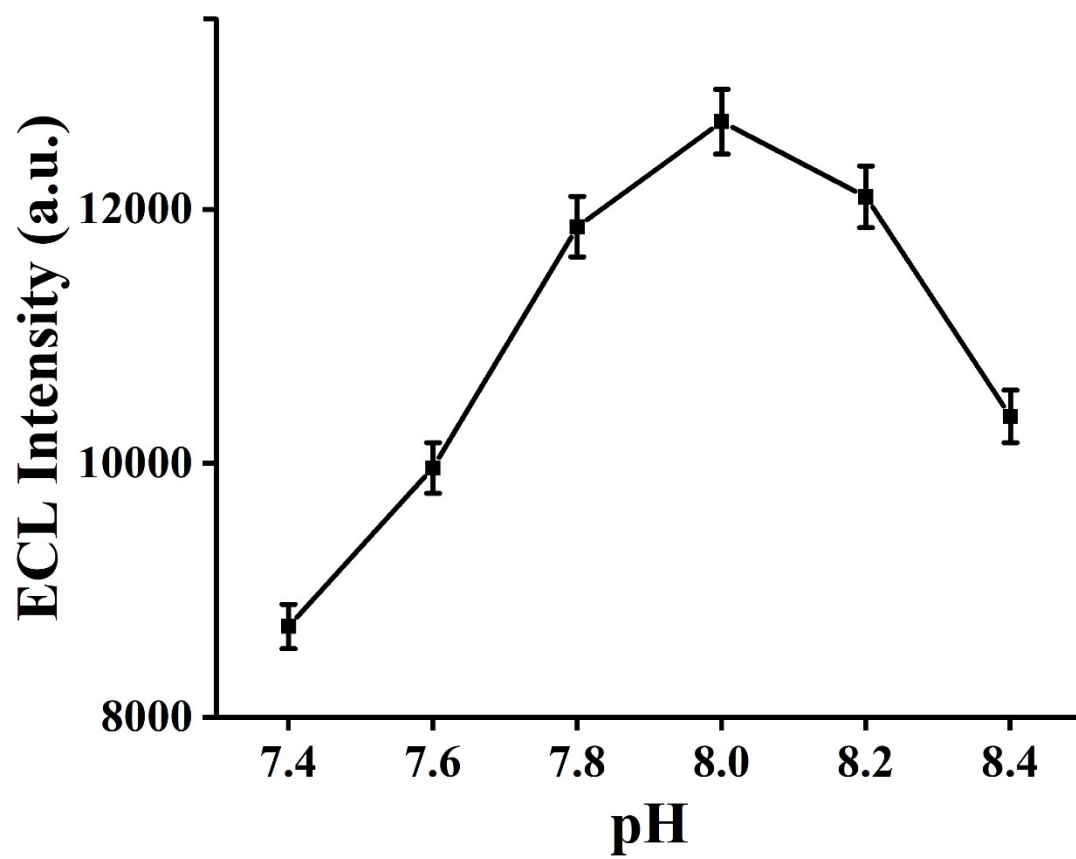


Fig. S4 ECL intensity under different pH of Tris-HCl. Error bars: SD ($n = 5$).

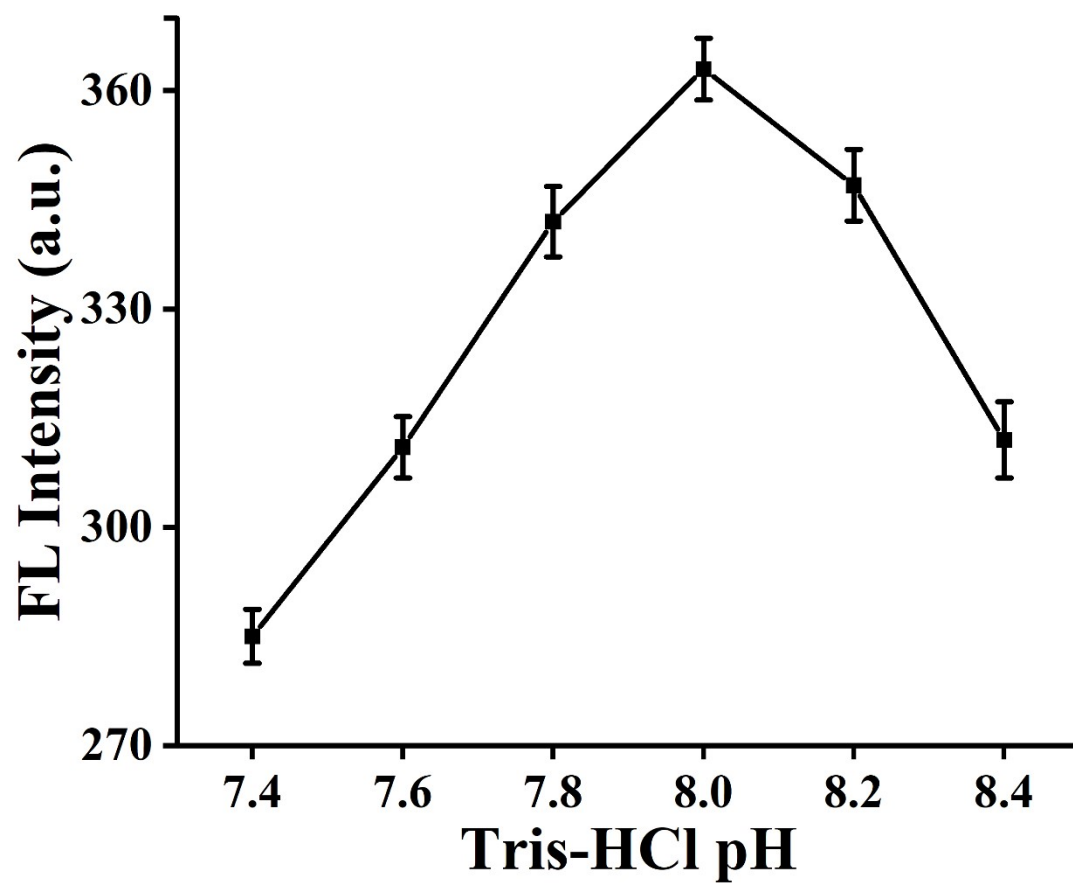


Fig. S5 FL intensity under different pH of Tris-HCl. Error bars: SD ($n = 5$).

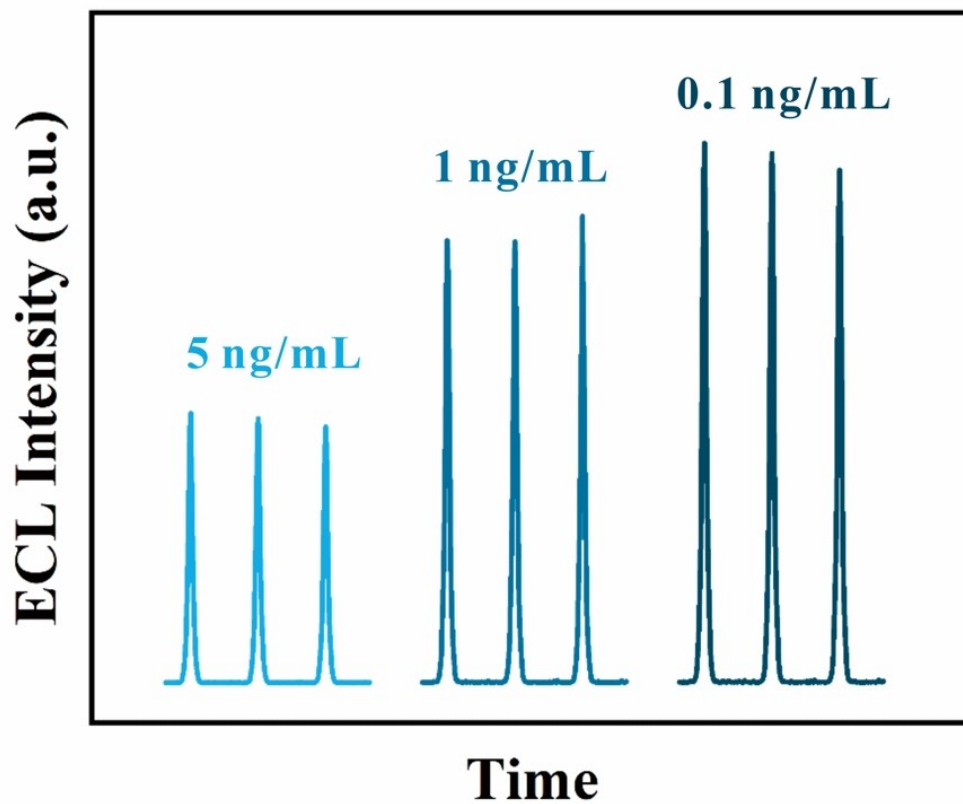


Fig. S6 The stability of the biosensor was tested under different LPS concentrations with three parallel measurements.

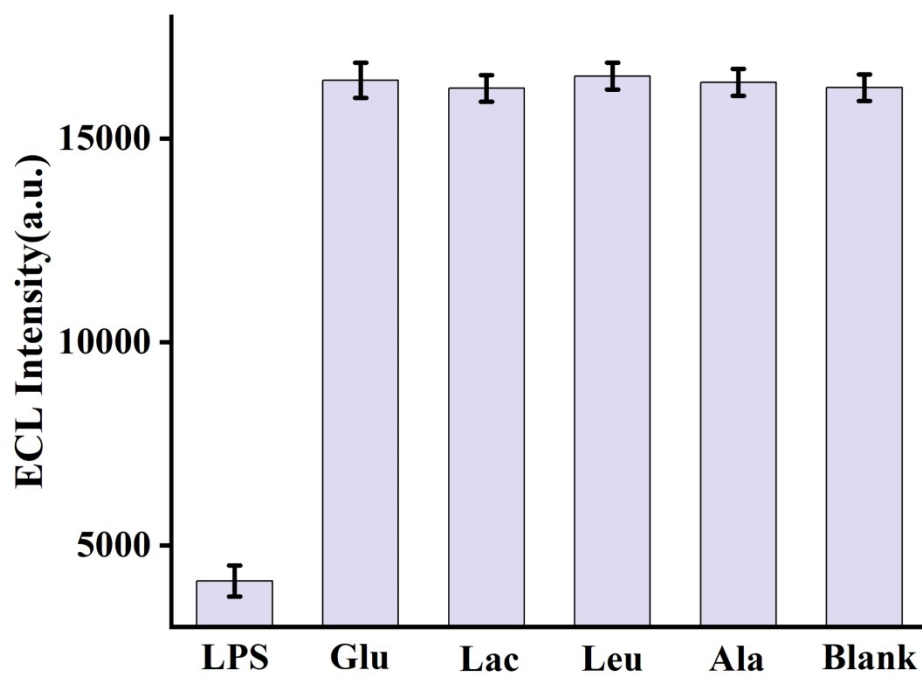


Fig. S7 Selectivity test under different substance interference (Glu, Lac, Leu, Ala, miR-200c, and blank). Error bars: SD ($n = 5$).

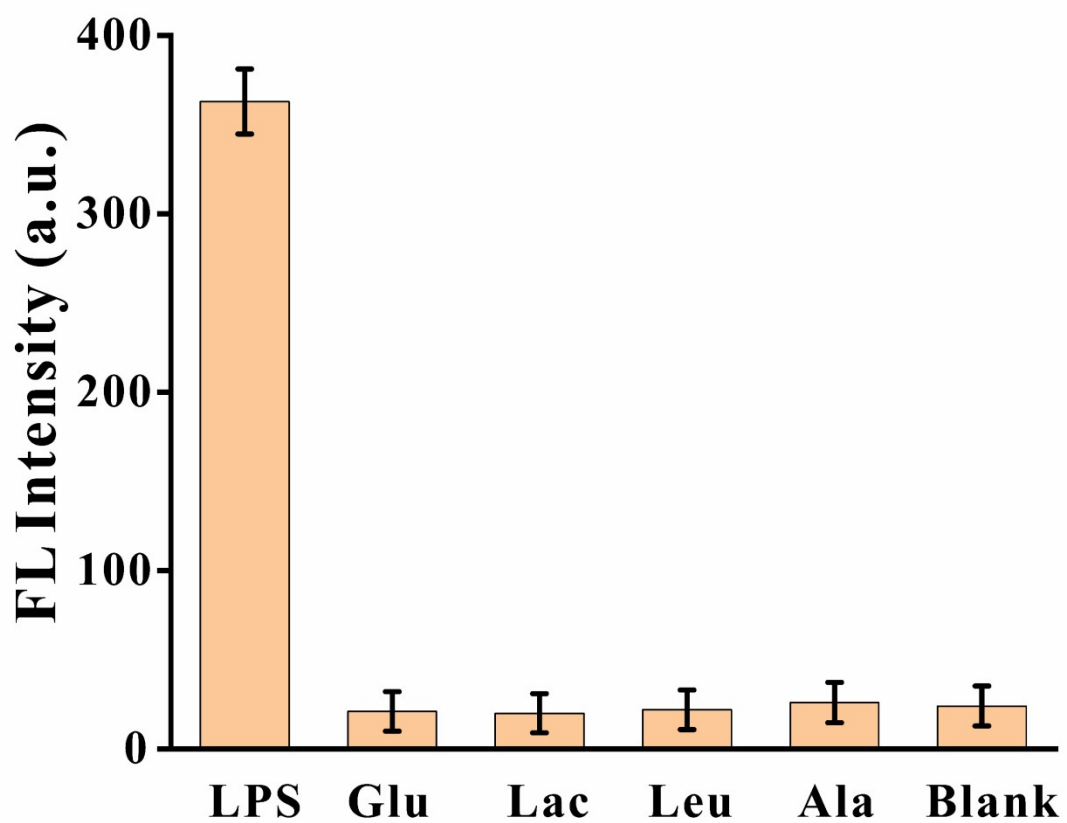


Fig. S8 Selectivity test under different substance interference (Glu, Lac, Leu, Ala, miR-200c, and blank). Error bars: SD ($n = 5$).

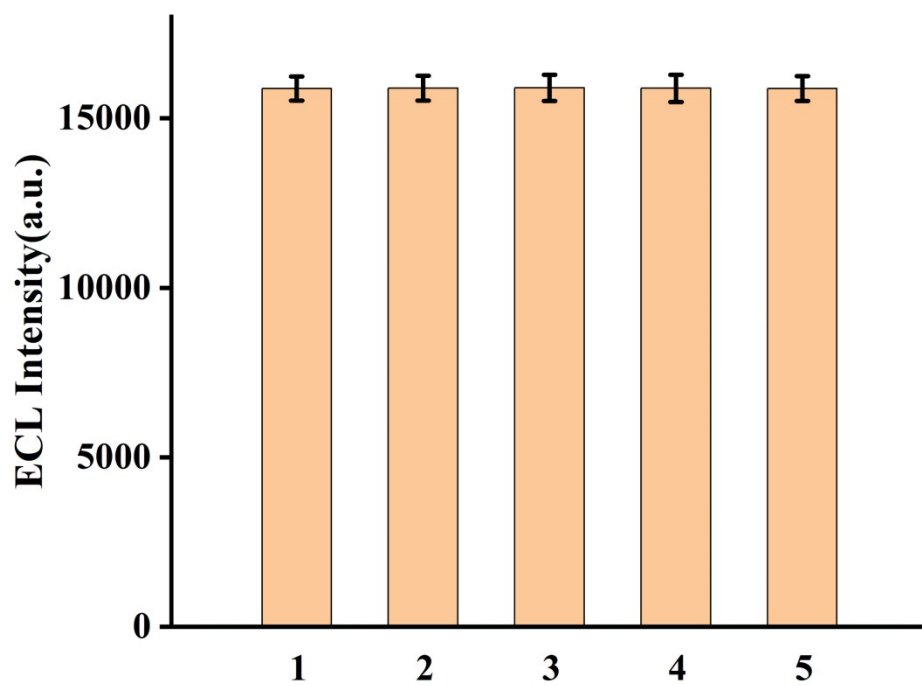


Fig. S9 Reproducibility of the ECL response to 0.01 ng/mL LPS spiked. Error bars: SD ($n = 5$).

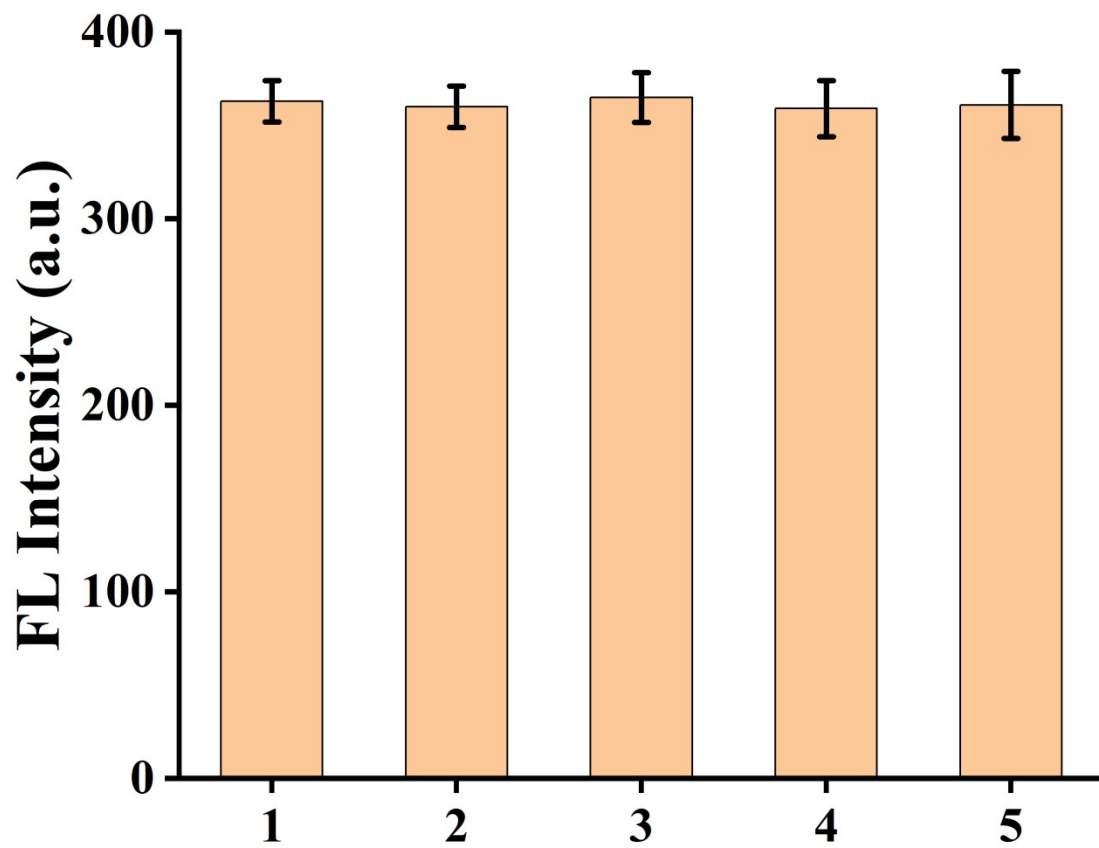


Fig. S10 Reproducibility of the FL response to 0.01 ng/mL LPS spiked. Error bars: SD ($n = 5$).

Table S1 Synthetic oligonucleotide sequences.

| Names | Sequences (5'-3') |
|-------|--|
| HP1 | GGGGAGGGTGGGGTGTTTAAGTTGGAGAATTGTACTTAAACACCTTCTT CTAGGGT |
| HP2 | AGGGTCAATTCTCCA ACTTAACTAGAGAAGGTGTTTAAGTAGGGG AGGGTGGGG |
| T | AGAAGAAGGTGTTTAAGTA |
| c-myc | AGGGTGGGGAGGGTGGGG |
| Apt | CTTCTGCCCGCCTCCTTCTAGCCGGATCGCGCTGGCCAGATGATATAA AGGGTCAGCCCCCAGGAGACGAGATAGGCGGACACT |
| crRNA | UAAUUUCUACUAAGUGUAGAUUAUCAUCUGGCCAGCGCGAU |

Table S2. Comparison of LPS analysis using other methods with the proposed dual-mode detection.

| Technique | Strategy | Detection range (ng/mL) | LOD (ng/mL) | Ref. |
|---|---|---|-----------------------|-----------|
| Electrochemical | Human Toll-Like Receptor-4 was immobilized on both a large area and micro gold electrode via the tethering interaction of a modified Self-Assembled Monolayer | 1.00 to 1.00×10^4 | 1.00 | 1 |
| Electrochemiluminescence | MoS ₂ Quantum Dots as New Electrochemiluminescence Emitters | 1.00×10^{-7} to 5.00×10^1 | 7.00×10^{-8} | 2 |
| Grating-coupled surface plasmon resonance | The sensor system relies on the smartphone's built-in flash light source and camera, a disposable sensor chip | 0 to 1.00×10^4 | 3.25×10^1 | 3 |
| Fluorescence | Boronic ester-mediated dual recognition has been coupled with a CRISPR/Cas12a system | 5.00×10^{-2} to 5.00×10^3 | 4.49×10^{-2} | 4 |
| Electrochemical | A miniaturized electrochemical cell sensor | 1.00×10^{-2} to 1.00×10^4 | 3.50×10^{-3} | 5 |
| Electrochemiluminescence and fluorescence | A CRISPR/Cas12a-powered nanoconfined biosensing system | 5.00×10^{-3} to 1.00×10^2 | 1.40×10^{-3} | This work |

Notes and references

1. R.M. Mayall, M. Renaud-Young, N.W.C. Chan and V.I. Birss, *Biosens. Bioelectron.* 2017, **87**, 794-807.
2. M. Zhao, A. Chen, D. Huang, Y. Chai, Y. Zhuo and R. Yuan, *Anal. Chem.* 2017, **89**, 8335–8342
3. J. Zhang, I. Khan, Q. Zhang, X. Liu, J. Dostalek, B. Liedberg and Y. Wang, *Biosens. Bioelectron.* 2018, **99**, 312-317.
4. A. Sheng, J. Yang, L. Cheng, and J. Zhang, *Anal. Chem.* 2022, **94**, 12523–12530.
5. H. Jiang, J. Yang, K. Wan, D. Jiang, and C. Jin, *ACS Sens.* 2020, **5**, 1325–1335.